HORIZONTAL STABILITY OF A QUASI–ZERO STIFFNESS MECHANISM USING INCLINED LINEAR SPRINGS

William S. P. Robertson, Ben Cazzolato, and Anthony Zander
School of Mechanical Engineering, The University of Adelaide, SA 5005, Australia

will.robertson@adelaide.edu.au

Negative stiffness mechanisms have seen renewed attention in recent years for their ability to reduce the resonance frequency of a structure without impeding their load-bearing ability. Such systems are often described as having quasi-zero stiffness when the negative stiffness is tuned to reduce the overall stiffness of the system as close to zero as possible without creating an instability. The system analysed in this work consists of a vertical spring for load bearing, and two symmetric inclined springs which behave with a snap-through effect to achieve negative stiffness. While this structure has been analysed extensively in the literature, generally only the stiffness in the vertical direction has been considered in the past. Here, the horizontal stiffness is assessed as well, and it is shown that it is possible to achieve quasi-zero stiffness in both directions simultaneously if the spring stiffnesses and pre-loads are chosen appropriately. Attention is paid to the tuning required in order to set the equilibrium point at a position which is arbitrarily close to having quasi-zero stiffness while avoiding issues arising from mechanical instability.

INTRODUCTION

In recent years a number of nonlinear systems have been proposed for vibration isolation to overcome the trade-off between low stiffness and high load bearing. These systems in general use a combination of positive and negative stiffness elements to achieve a localised region of 'quasi–zero stiffness' at or near the equilibrium position of the system [13].

One system that exemplifies this idea involves using a repelling magnet pair to provide load bearing and an attracting magnet pair to provide negative stiffness which has been investigated previously by the present authors [10, 16, 11]. The noncontact forces of the magnetic system make them well-suited for online tuning [15, 14], but the inherent instability of magnetic systems can add complexity to the control required.

While flexible structures have been shown to operate similarly [12, 4, 7], the most common system for achieving quasi–zero stiffness involves arrangements of inclined mechanical springs which generally operate in 'snap-through' regimes such as the spring arrangement shown in Figure 1 [8, 3, 2]. This system consists of a load bearing vertical spring in parallel with a pair of inclined springs that behave in a buckling regime. Generally, analyses of this system have only considered its stiffness properties in a single degree of freedom, in the direction of the primary load bearing.

This paper consists of an analysis of the quasi-static behaviour of this inclined spring system and re-formulates the force and stiffness characteristics in both vertical and horizontal directions, describing in some detail the approach by which low stiffness in both directions can be achieved. Low stiffness in the vertical direction has been previously documented due to the negative vertical stiffness of a pair of horizontal springs in compression. Low stiffness in the horizontal direction is newly analysed here, which is achieved due to the negative stiffness in the horizontal direction of the load-bearing vertical spring.

This publication is based on the paper that was awarded the President's Prise at the 2013 Australian Acoustical Society Conference.

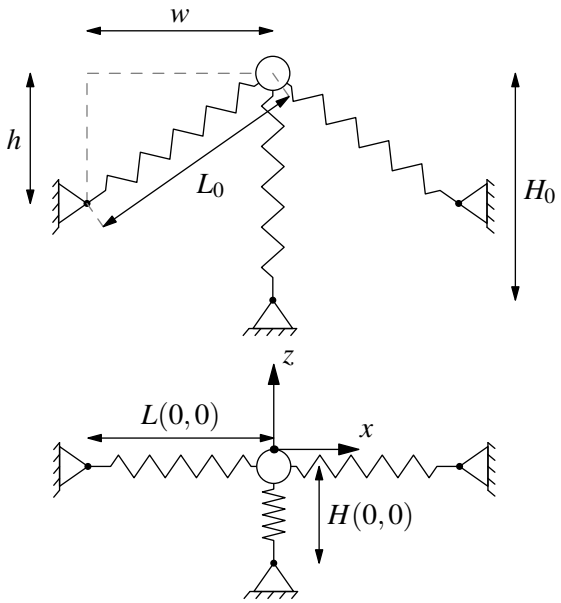

Figure 1. Negative stiffness inclined springs in parallel with a positive stiffness spring. Top: the system with the inclined springs in their uncompressed state corresponding to a vertical displacement of $z = h$. Bottom: inclined springs at a position of maximum negative stiffness, corresponding to a vertical displacement of $z = 0$

GEOMETRY

Figure 1 shows the planar inclined spring system both without load (that is, with undeflected springs) and after deflection to

the position which has the potential of achieving 'quasi–zero stiffness', which is the position of maximum compression of the inclined springs. The overall stiffness of the system must be tuned to support the mass of the load at this position.

At the unloaded state shown in Figure 1, all springs are considered to be in their uncompressed state; with inclined spring lengths $L_0 = \sqrt{h^2+w^2}$ and vertical spring length $H_0 = \eta L_0$, where η is denoted the 'length ratio' between the vertical and inclined springs. The inclined springs each have stiffness k_i and the vertical spring has stiffness $k_v = \alpha k_i$, with α denoted the 'stiffness ratio' between the vertical and inclined springs. The stiffness and deflection properties of the springs are summarised in Table 1.

The position at which the inclined springs are horizontal defines the displacement origin of the system, where z is the displacement in the load bearing direction, and x is the displacement in the non–load bearing direction (this is used later for the derivation of the horizontal stiffness of the system).

The deflected lengths of the springs from vertical displacement z and horizontal displacement x are $L(x,z)$ for the inclined spring and $H(x,z)$ for the vertical spring. The compressed length of the inclined spring on the left is

$$L(x,z) = \sqrt{[w+x]^2+z^2}, \tag{1}$$

and the vertical spring length is

$$H(x,z) = \sqrt{x^2+[H_0-h+z]^2}; \tag{2}$$

note that $L(0,h) = L_0$ and $H(0,h) = H_0$.

The geometry that has been chosen uses linear springs that are all arranged to be undeflected in the unloaded state of the system. Kovacic, Brennan, and Waters [6] have explored the effects of including pretension and the use of nonlinear softening springs for vertical vibration isolation.

VERTICAL FORCES

The forces on the mass are calculated by analysing the components due to each spring individually. The force due to the inclined spring (on the left of Figure 1), in the direction of the spring, is given by

$$F_i(x,z) = [L_0 - L(x,z)]\,k_i = \left[\sqrt{w^2+h^2} - \sqrt{[w+x]^2+z^2}\right] k_i. \tag{3}$$

Assuming only vertical displacement ($x = 0$), the vertical component of this inclined spring force is

$$F_{i_v}(0,z) = F_i(0,z)\frac{z}{L(0,z)} = zk_i\left[\frac{\sqrt{w^2+h^2}}{\sqrt{w^2+z^2}} - 1\right]. \tag{4}$$

It is convenient to normalise this result by representing the lengths and displacements as ratios of the uncompressed height of the inclined springs. With the coordinate substitutions

Table 1. Properties of the springs in the quasi–zero stiffness inclined spring system defining stiffness ratio α and length ratio η.

Spring	Stiffness	Undeflected length
Inclined	k_i	$L_0 = \sqrt{h^2+w^2} = \sqrt{h^2\,[1+\gamma^2]}$
Vertical	$k_v = \alpha k_i$	$H_0 = \eta L_0$

$\xi = z/h$ and $\gamma = w/h$, the inclined spring force in the vertical direction can be written in non-dimensional form as

$$\frac{F_{i_v}(\xi)}{hk_i} = \xi\left[\sqrt{\frac{\gamma^2+1}{\gamma^2+\xi^2}} - 1\right], \tag{5}$$

where γ is denoted the 'geometric ratio' of the device and ξ the normalised displacement. Note that here $\gamma = 0$ corresponds to unloaded inclined springs at 90° (that is, vertical) before compression, and $\gamma = \infty$ corresponds to unloaded inclined springs at 0° (that is, horizontal). In the coordinate system used here, the displacement origin $z = 0$ corresponds to the position of maximum compression of the inclined springs; that is, when they are horizontal.

Figure 2 illustrates the force characteristic of Eq. (5) versus normalised displacement for a range of geometric ratios γ. In Figure 2 and later figures, the geometric ratio γ is expressed as a ratio of γ^*, the value of γ that produces quasi–zero stiffness for this system; γ^* will be derived later in Eq. (12). The 'snap-through' forces that cause the negative stiffness are especially strong for smaller values of geometric ratio γ (that is, the more vertical the spring angles before deflection).

The total vertical force produced by the system, $F_{t_v}(x,z)$, is calculated by combining Eq. (4) for each inclined spring with the force due to the vertical spring:

$$F_{t_v}(x,z) = 2F_{i_v}(x,z) + F_{v_v}(x,z)\,. \tag{6}$$

For vertical displacements, the force due to the vertical spring is given by

$$F_{v_v}(x,z) = [h-z]\,k_v\,, \tag{7}$$

and the total force in the vertical direction can be nondimensionally represented by

$$\frac{F_{t_v}(x,z)}{hk_i} = -\xi\alpha + \alpha + 2\xi\left[\sqrt{\frac{\gamma^2+1}{\gamma^2+\xi^2}} - 1\right], \tag{8}$$

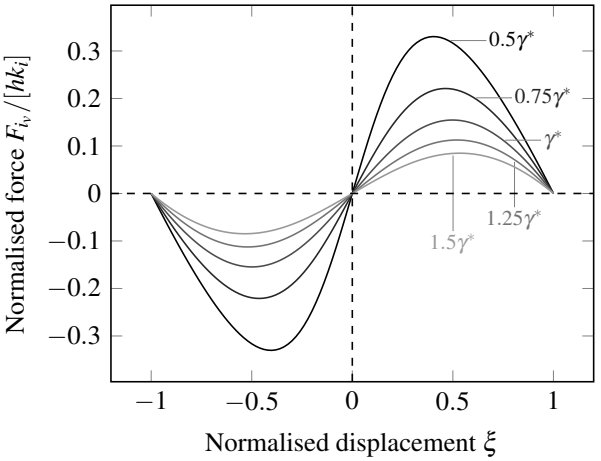

Figure 2. Vertical force due to inclined springs only for a range of geometric ratios γ.

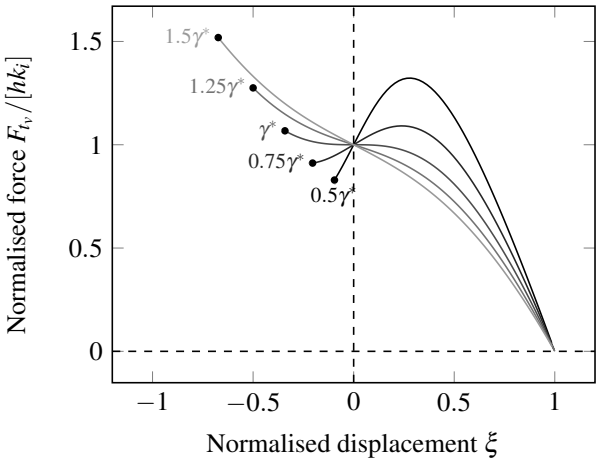

Figure 3. Normalised vertical force characteristic of the system calculated with Eq. (8).

recalling that $\alpha = k_v/k_i$ is the stiffness ratio between the vertical and inclined springs. This equation is depicted in Figure 3 for a unity stiffness ratio ($\alpha = 1$), where it can be seen that by selecting the geometric ratio γ appropriately it is possible to generate a local region of low stiffness at displacement $\xi = 0$, approaching the quasi–zero stiffness condition under ideal circumstances. The calculation for γ^*, the value of the geometric ratio γ for which quasi–zero stiffness is achieved, will be shown later in Eq. (12).

The force curves in Figure 3 terminate at a certain point in the negative displacement region, which corresponds to the maximum possible compression of the vertical spring, given by the condition $H(0, z_{\min}) = 0$. In other words, the spring has been compressed to zero length. This condition can be solved for $z_{\min}$ and subsequently normalised for the equivalent $\xi_{\min}$, which are given by

$$z_{\min} = h - H_0, \qquad \xi_{\min} = 1 - \eta\sqrt{\gamma^2 + 1}. \tag{9}$$

VERTICAL STIFFNESSES

The vertical stiffness characteristic, K_v, of the system is calculated by differentiating the vertical force, Eq. (8), with respect to vertical displacement z, yielding

$$K_v = -\frac{\mathrm{d}}{\mathrm{d}z} F_{t_v}(x, z)\,, \tag{10}$$

which can be written in non-dimensional form as

$$\frac{K_v}{k_i} = -2\gamma^2 \sqrt{\frac{\gamma^2 + 1}{[\gamma^2 + \xi^2]^3}} + \alpha + 2\,. \tag{11}$$

Graphs of the normalised vertical stiffness K_v/k_i versus normalised displacement ξ are shown in Figure 4 for a range of geometric ratios γ, which show that the stiffness at $\xi = 0$ varies from negative to positive as γ increases. The parameter selection required to achieve a quasi–zero stiffness condition in the vertical direction can be found by solving Eq. (11) for $K_v = 0$ at $\xi = 0$. This results in the relation

$$\gamma^* = \frac{2}{\sqrt{\alpha^2 + 4\alpha}} \tag{12}$$

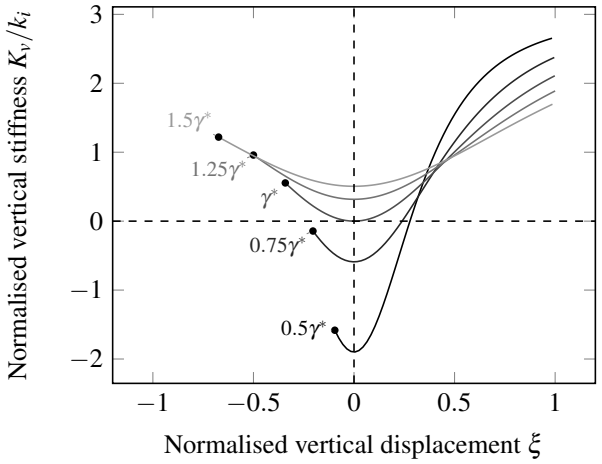

Figure 4. Vertical stiffness characteristic for a range of geometric ratios γ at $\alpha = 1$, calculated with Eq. (11).

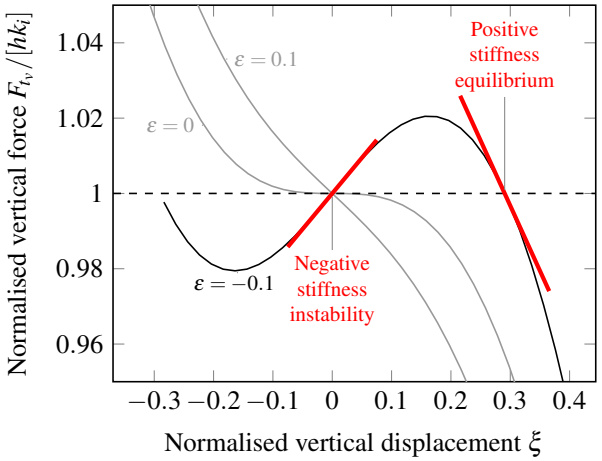

Figure 5. The stable and unstable equilibrium points of the inclined spring system near quasi–zero stiffness for $\varepsilon \in \{-0.1, 0, 0.1\}$. The rest position will move from the unstable point to the stable point of equilibrium.

which is used as the reference value of the geometric ratio γ for the results shown in Figures 2, 3, 4 and 7.

Achieving exactly quasi–zero stiffness with this spring is not feasible in practice as the stiffness characteristic becomes negative for $\gamma < \gamma^*$, as shown in Figure 4. This is important as the geometric ratio γ will have some uncertainty in its value due to environmental conditions such as temperature and physical imperfections such as creep. The deviation of γ from γ^*, ε, can be defined by

$$\gamma = [1 + \varepsilon]\,\gamma^*. \tag{13}$$

Figure 5 shows the total vertical force, F_{t_v}, of the system for $\varepsilon \in \{-0.1, 0, 0.1\}$. It can be seen that negative values of ε (that is, a geometric ratio less than that for quasi–zero stiffness) correspond to negative stiffness at normalised displacement $\xi = 0$. A system in this condition is in a position of unstable equilibrium, and will move towards and remain at the position of stable equilibrium indicated in the figure rather than the design point at $\xi = 0$.

Figure 6 plots the stiffness at this deviated equilibrium point as ε varies; in the unstable zone, the system will move to the equilibrium point shown in Figure 5 away from $\xi = 0$. (With

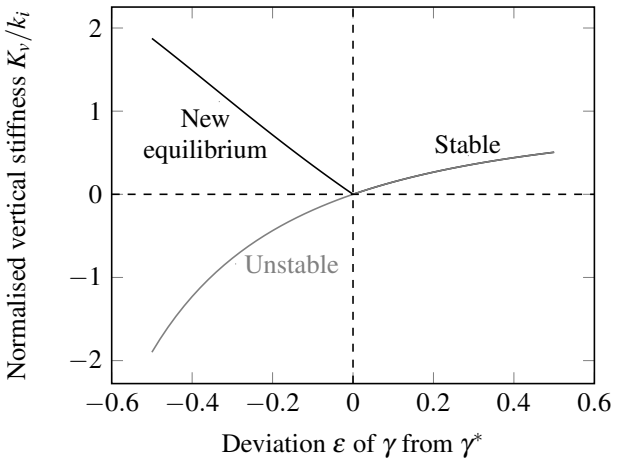

Figure 6. The stiffness at equilibrium as ε varies; as the stiffness becomes negative, the stiffness shown corresponds to the stable point of equilibrium shown in Figure 5.

sufficient excitation the system will 'snap though' from one equilibrium position to another with a resulting displacement profile that is comparatively large given the excitation amplitude; this mechanism has been proposed as a useful phenomenon for energy harvesting purposes [9].) It can be seen that the stiffnesses in the stable region for $\varepsilon > 0$ are smaller than the stiffnesses in the equilibrium region for $\varepsilon < 0$. This highlights the importance of never breaching the $\varepsilon < 0$ instability condition. Therefore, a chosen value for the geometric ratio γ will approach γ^* but always be slightly greater in order to retain stability of the equilibrium position.

HORIZONTAL STIFFNESS CHARACTERISTIC DUE TO VERTICAL DISPLACEMENT

Now that the vertical stiffness characteristics of the system have been analysed and a condition derived to achieve quasi–zero stiffness in that direction, the same approach will be taken for the horizontal behaviour. Only vertical displacements will be considered in assessing the horizontal stability. This can be justified by considering how instability in the horizontal direction arises: as the vertical spring is compressed it generates lateral forces as the load becomes off-centre. These lateral forces correspond to a negative stiffness that has greatest magnitude for zero horizontal displacement, and therefore for a position of stable equilibrium a small deviation will not result in sudden instability.

In order to calculate the horizontal stiffness of the system, the force from the vertical spring needs to be represented in terms of both vertical and horizontal displacements. This force, aligned in the direction of the nominally-vertical spring, is

$$F_v(x,z) = \left[\eta L_0 - \sqrt{x^2 + [-h+z+\eta L_0]^2}\right] k_v, \tag{14}$$

recalling that x is the displacement of the mass in the horizontal direction. Substituting $x = 0$ into Eq. (14) yields the previous Eq. (7). The horizontal component of this force is

$$F_{v_h}(x,z) = F_v(x,z)\frac{x}{H(x,z)}\,. \tag{15}$$

Similarly, the horizontal component of the force from the inclined spring on the left (referring to Figure 1) is given by

$$F_{i_h}(x,z) = F_i(x,z)\frac{w+x}{L(x,z)}\,, \tag{16}$$

and the horizontal component of the force from the inclined spring on the right is

$$F_{i_h}(x,z)\Big|_{\text{right}} = -F_{i_h}(-x,z)\,. \tag{17}$$

The stiffness characteristic in the horizontal direction, K_h, is derived in a similar fashion to the vertical stiffness. The total force in the horizontal direction is

$$F_{l_h}(x,z) = F_{i_h}(x,z) - F_{i_h}(-x,z) + F_{v_h}(x,z)\,. \tag{18}$$

Differentiating with respect to horizontal displacement x and evaluating at $x = 0$ gives the horizontal stiffness characteristic as the vertical displacement varies,

$$\frac{K_h}{k_i} = -2\xi^2\sqrt{\frac{\gamma^2+1}{[\gamma^2+\xi^2]^3}} + \frac{\alpha\,[\xi-1]}{\eta\sqrt{\gamma^2+1}+\xi-1} + 2. \tag{19}$$

This horizontal stiffness is shown in Figure 7 as a function of vertical displacement. Comparing this to the vertical stiffness results (Figure 4), it can be seen that while the vertical stiffness is zero at normalised displacement $\xi = 0$ and geometric ratio $\gamma = \gamma^*$ (which is as derived), the horizontal stiffness exhibits separate behaviour, and can even be negative (that is, unstable) for values of γ lower than around $1.25\gamma^*$.

Since the vertical stiffness and horizontal stiffness are independent, further analysis into the behaviour of the horizontal stiffness at the vertical quasi–zero stiffness condition is warranted. Substituting the quasi–zero stiffness condition of Eq. (12) into Eq. (19) at displacement $\xi = 0$ gives the normalised horizontal stiffness as a function of stiffness ratio α:

$$\frac{K_h}{k_i}\Big|_{\text{V. QZS}} = 2 - \alpha\left[\frac{[\alpha+2]\,\eta}{\sqrt{\alpha\,[\alpha+4]}} - 1\right]^{-1}. \tag{20}$$

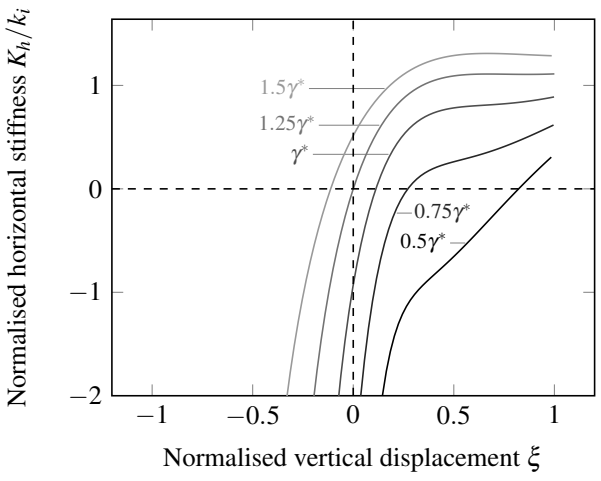

Figure 7. Horizontal stiffness characteristic for a range of geometric ratios γ at $\alpha = 1$, calculated with Eq. (19).

This equation is depicted in Figure 8; it can be seen that the horizontal stiffness of the spring may be chosen by varying both the spring stiffness ratio α and the spring length ratio η. Since the length ratio η is not found in Eq. (11), the horizontal and vertical stiffnesses may be tuned independently in order to achieve quasi–zero stiffness in both simultaneously.

To obtain zero stiffness in the horizontal direction at the nominal position, Eq. (20) is solved for $K_h = 0$, showing a relationship between α and η when the quasi–zero stiffness condition is achieved in both the vertical and the horizontal directions.

$$\begin{aligned} \alpha^*(\eta) &= 2\left[\sqrt{\eta^2+1}-1\right], \text{ or} \\ \eta^*(\alpha) &= \frac{1}{2}\sqrt{\alpha\,[\alpha+4]}. \end{aligned} \tag{21}$$

As a consequence, increasing η (say, in order to reduce the compression of the vertical spring) results in an increasing value of the vertical spring stiffness in order to remain at quasi–zero stiffness.

Using α^* from Eq. (21) in the stiffness equations (11) and (19) allows the stiffness characteristics of the system in the two directions to be compared when both have quasi–zero stiffness simultaneously. Considering the vertical stiffness first in Figure 9, it can be seen that increasing the length ratio η increases the vertical stiffness gradient, which is an important parameter to be kept small in order to mitigate possible nonlinear dynamic effects that may arise due to a large rate of change of stiffness over displacement.

The graph of horizontal stiffness versus vertical displacement is shown in Figure 10. Note that contrary to the vertical case, the horizontal stiffness curves are not symmetric around zero vertical displacement. This is caused by the effect of the vertical spring; with negative vertical displacement (compression of the vertical spring) a horizontal perturbation results in an unstable horizontal force, whereas with positive vertical displacement (extension of the vertical spring) any horizontal forces act in a restoring sense.

Figure 10 illustrates that the quasi–zero stiffness condition is always marginally unstable in the horizontal direction since negative vertical displacement will result in negative horizontal stiffness. In practice this requires that the system be tuned slightly away from the quasi–zero stiffness condition in the horizontal direction after accommodating for the maximum disturbance displacement of the isolator. It is possible to do this without compromising the quasi–zero stiffness condition in the vertical direction because the spring length ratio η does not affect the vertical stiffness.

As an example, Figure 11 shows the horizontal stiffness for a stiffness ratio detuned by five percent below that required for quasi–zero stiffness (that is, $\alpha = 0.95\alpha^*$). In comparison with Figure 10, the spring has a stable displacement range of approximately $\xi = \pm 0.025$. Provided that the spring length ratio η is large enough, the horizontal stiffness at $\xi = 0$ is still significantly reduced.

Therefore, there is a direct compromise between the nonlinearity of the stiffness in the vertical direction (which

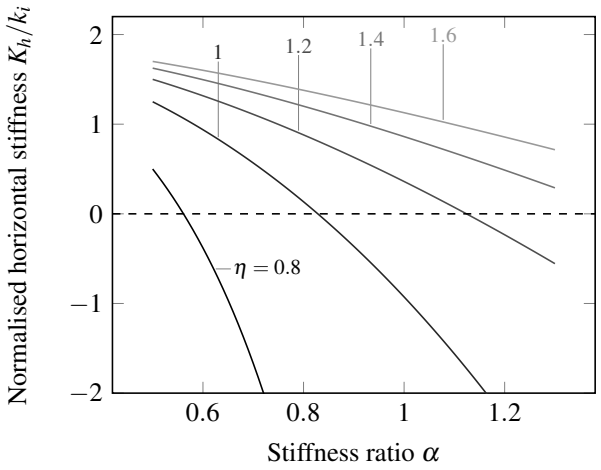

Figure 8. Horizontal stiffness characteristic versus stiffness ratio α at the vertical quasi–zero stiffness condition for varying length ratio η, calculated with Eq. (20).

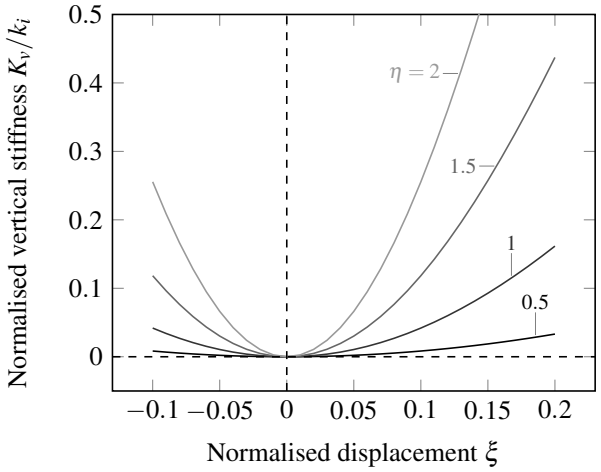

Figure 9. Vertical stiffness characteristics at quasi–zero stiffness in both directions, for a range of spring length ratios η.

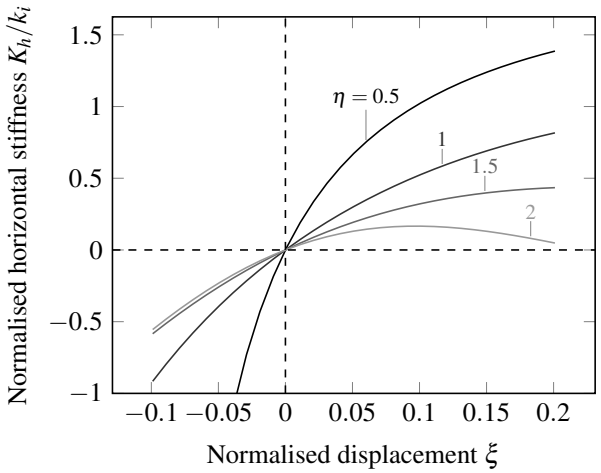

Figure 10. Horizontal stiffness characteristics at quasi–zero stiffness in both directions, for a range of spring length ratios, η. Note that negative displacement will result in negative stiffness.

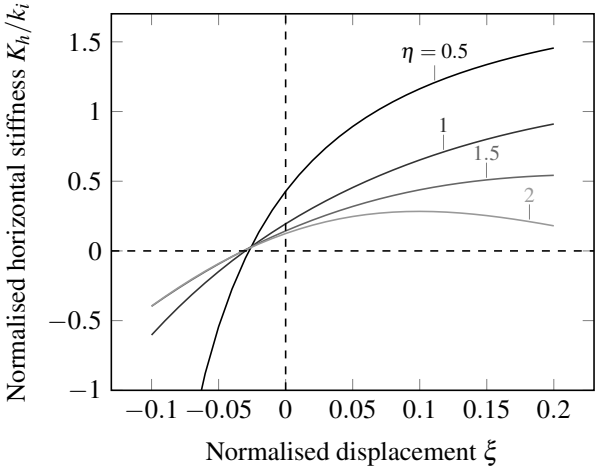

Figure 11. Normalised horizontal stiffness of the system at $\alpha = 0.95\alpha^*$ in order to obtain a small range of displacement around $\xi = 0$ with positive stiffness. The vertical quasi–zero stiffness condition is unaffected.

increases with η) and the amount of stiffness reduction in the horizontal direction (which decreases with η).

CONCLUSION

This paper has analysed the horizontal stiffness characteristics of a common quasi–zero stiffness arrangement that uses linear mechanical springs. This system has been analysed extensively in the literature with respect to its vertical stiffness properties and its suitability for vibration isolation; this work has shown that with correctly tuned spring stiffnesses, low horizontal stiffness can be achieved simultaneously with low vertical stiffness.

REFERENCES

[1] P. Alabuzhev, A. Gritchin, L. Kim, G. Migirenko, V. Chon, and P. Stepanov. *Vibration Protecting and Measuring Systems with Quasi-Zero Stiffness*. Ed. by E. Rivin. Applications of Vibration. Hemisphere Publishing Corporation, 1989. ISBN: 0-89116-811-7.

[2] A. Carrella, M. J. Brennan, I. Kovacic, and T. P. Waters. "On the force transmissibility of a vibration isolator with quasi-zero-stiffness". *Journal of Sound and Vibration* 322.4–5 (May 2009), pp. 707–717.

[3] A. Carrella, M. J. Brennan, and T. P. Waters. "Static analysis of a passive vibration isolator with quasi-zero-stiffness characteristic". *Journal of Sound and Vibration* 301.3–5 (Apr. 2007), pp. 678–689.

[4] G. Cella, V. Sannibale, R. DeSalvo, S. Marka, and A. Takamori. "Monolithic geometric anti-spring blades". *Nuclear Instruments and Methods in Physics Research Section A: Accelerators, Spectrometers, Detectors and Associated Equipment* 540.2-3 (2005), pp. 502–519.

[5] J. Choi, S. Hong, W. Lee, S. Kang, and M. Kim. "A Robot Joint With Variable Stiffness Using Leaf Springs". *IEEE Transactions on Robotics* 27.2 (Apr. 2011), pp. 229–238.

[6] I. Kovacic, M. J. Brennan, and T. P. Waters. "A study of a nonlinear vibration isolator with a quasi-zero stiffness characteristic". *Journal of Sound and Vibration* 315.3 (2008), pp. 700–711.

[7] C.-M. Lee, V. N. Goverdovskiy, and A. I. Temnikov. "Design of springs with "negative" stiffness to improve vehicle driver vibration isolation". *Journal of Sound and Vibration* 302.4–5 (May 2007), pp. 865–874.

[8] W. G. Molyneux. *Supports for vibration isolation*. ARC/CP-322. Aeronautical Research Council, Great Britain, 1957.

[9] R. Ramlan, M. Brennan, B. Mace, and I. Kovacic. "Potential benefits of a non-linear stiffness in an energy harvesting device". *Nonlinear Dynamics* 59.4 (Mar. 2009), pp. 545–558.

[10] W. S. Robertson, M. R. F. Kidner, B. S. Cazzolato, and A. C. Zander. "Theoretical design parameters for a quasi-zero stiffness magnetic spring for vibration isolation". *Journal of Sound and Vibration* 326.1–2 (2009), pp. 88–103.

[11] W. S. P. Robertson, B. Cazzolato, and A. Zander. "Experimental results of a 1D passive magnetic spring approaching quasi-zero stiffness and using active skyhook damping". *Proceedings of Acoustics 2013*. Victor Harbor, Australia, Nov. 2013.

[12] T. Tarnai. "Zero stiffness elastic structures". *International Journal of Mechanical Sciences* 45.3 (Mar. 2003), pp. 425–431.

[13] J. T. Xing, Y. P. Xiong, and W. G. Price. "Passive-active vibration isolation systems to produce zero or infinite dynamic modulus: Theoretical and conceptual design strategies". *Journal of Sound and Vibration* 286.3 (2005), pp. 615–636.

[14] D. Xu, Q. Yu, J. Zhou, and S. Bishop. "Theoretical and experimental analyses of a nonlinear magnetic vibration isolator with quasi-zero-stiffness characteristic". *Journal of Sound and Vibration* 332.14 (July 2013), pp. 3377–3389.

[15] N. Zhou and K. Liu. "A tunable high-static-low-dynamic stiffness vibration isolator". *Journal of Sound and Vibration* 329.9 (2010), pp. 1254–1273.

[16] T. Zhu, B. Cazzolato, W. Robertson, and A. Zander. "The development of a 6 degree of freedom quasi-zero stiffness maglev vibration isolator with adaptive-passive load support". *15th International Conference on Mechatronics Technology*. 2011.